Biomedical Engineering Letters (2024) 14:1195–1205
https://doi.org/10.1007/s13534-024-00423-x

REVIEW ARTICLE

Monte Carlo methods for medical imaging research

Hoyeon Lee[1]

Received: 15 April 2024 / Revised: 24 July 2024 / Accepted: 26 August 2024 / Published online: 5 September 2024

Abstract
In radiation-based medical imaging research, computational modeling methods are used to design and validate imaging systems and post-processing algorithms. Monte Carlo methods are widely used for the computational modeling as they can model the systems accurately and intuitively by sampling interactions between particles and imaging subject with known probability distributions. This article reviews the physics behind Monte Carlo methods, their applications in medical imaging, and available MC codes for medical imaging research. Additionally, potential research areas related to Monte Carlo for medical imaging are discussed.

Keywords Monte Carlo · Medical imaging · Computational modeling

1 Introduction

Medical images play a pivotal role in clinical settings as they provide anatomical and functional information about the human body without invasive procedures [1]. Radiation-based imaging devices, i.e., Computed Tomography (CT), Positron Emission Tomography (PET), and Single Photon Emission Computed Tomography (SPECT), are commonly used in clinical environments [2]. Recently developed imaging modalities, such as spectral CT, tomosynthesis, and breast CT, provide additional information to aid clinical decisions. Medical imaging devices have expanded their applications for image-guided radiotherapy (IGRT) for patient setup, dose verification, and treatment monitoring. This includes Cone-Beam CT (CBCT), Mega-Voltage CT (MVCT), In-beam PET, and Prompt Gamma imaging [3?6].

Numerous studies have been conducted to improve image quality and develop novel imaging modalities. The quality and information provided by the images are the basis of clinical decisions. Computational modeling offers safe and efficient means of obtaining realistic data and understanding radiation physics. Monte Carlo (MC) methods have been widely used in computational modeling of medical imaging studies and provide valuable insights for research and development [7].

In this article, we review the background on MC methods, their applications in medical imaging research, and commonly used codes in medical imaging research. In addition, potential research areas will be briefly discussed.

2 Physics background in MC

Radiation-based medical imaging modalities employ various radiation sources depending on the purpose. For instance, X-ray CT and tomosynthesis use photons generated by X-ray tubes, PET measures photons created by the annihilation of positrons, and SPECT utilizes gamma rays produced by radioactive decay. Although these modalities involve different radiation sources, the interactions of the particles with media are governed by the Linear Boltzmann Transport Equation (LBTE) as shown in Eq. (1) [8, 9]. The equation describes the behavior of particles in a small volume ΔV around r. In the equation, r is the position of particles, Ω is the traveling direction of particles, E is the energy of particles, ϕ is fluence of particles, S is the source term of particles, σ is the total cross-section, and σ_s is the differential cross-section of materials for particles.

The first term of the equation represents the fluence of particles with energy E and direction Ω ((E, Ω)) traveling ΔV without interaction. The second term accounts for the removal of particles with (E, Ω) due to absorption or

✉ Hoyeon Lee
hlee01@hku.hk

[1] Department of Diagnostic Radiology and Centre of Cancer Medicine, University of Hong Kong, Hong Kong, China

scattering in ΔV. The third term depicts the production of particles with (E, Ω) in ΔV. The fourth term describes the transition of particles from $(E\prime, \Omega\prime)$ to (E, Ω) in ΔV.

$$(\Omega \cdot \nabla)\phi(r, E, \Omega) + \sigma(r, E)\phi(r, E, \Omega) = S(r, E, \Omega) + \int_0^{E_0} dE \int_{4\pi} d\Omega[\sigma_s(r, E\prime \rightarrow E, \Omega' \rightarrow \Omega)\phi(r, E', \Omega')] \quad (1)$$

By solving the equation, one can transport particles and determine their energy, direction, and the number of particles that reach the detector.

The MC methods offer stochastic solutions to the equation by tracking a multitude of particles. For a given set of geometric components, particle types, and physics data, the MC methods randomly sample interactions between particles and geometric components based on cross-section data. This determines the interaction type, scattering angle, energy loss, and secondary particle generation. The particles are transported until they lose all their energy or are captured by the detector, as shown in Fig. 1. When particles are detected, signal-processing algorithms are applied to produce image data. This process is analogous too converting incoming particles into human-readable signals in experimental systems.

MC methods sample particle interaction with the geometric setup of imaging objects and imaging devices. Figure 2a depicts a CBCT detector based on the Varian On-Board Imager (OBI) system [10] (Varian Medical Systems, Palo Alto, CA, USA) and a numerical 3D Shepp-Logan phantom [11]. Figure 2b shows a PET detector based on GE Discovery MI [12] and the American College of Radiology (ACR)-type phantom [13] used for quality assurance (QA) of PET systems. The geometries and phantoms are built using TOol for PArticle Simulation (TOPAS) [14, 15] and TOPAS-imaging extension [16], which will be discussed later.

The accuracy of the solutions obtained from MC methods hinges on the precise modeling of imaging systems and imaging subjects, the physics processes involved, and the number of particles tracked, which determines the statistical uncertainties of the results. Generally, achieving lower statistical uncertainty requires significant computational cost. To optimize the balance between reducing uncertainty and managing computational demands, variance reduction techniques (VRTs), i.e., Russian roulette, particle splitting, and optical spread function, are frequently utilized in MC methods [17?20].

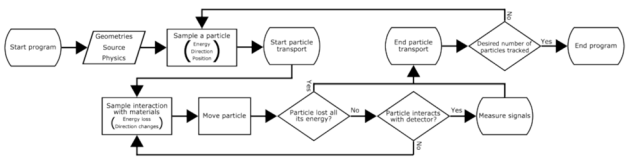

Fig. 1 Flowchart of MC simulations

3 MC applications in medical imaging research

3.1 Dosimetry

In radiation-based imaging, it is essential to estimate the potential risk to patients by calculating the radiation dose exposed during imaging [21]. Consequently, extensive studies have been conducted to develop dose calculation algorithms for imaging.

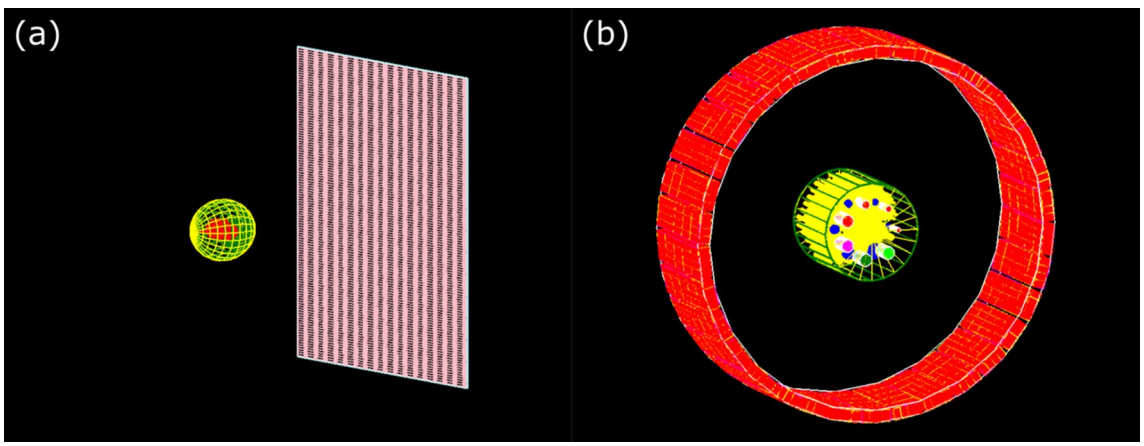

Fig. 2 Illustration of **a** CBCT detector and Shepp-Logan phantom and **b** PET detection system and ACR-type phantom

For CT dosimetry, the CT dose index (CTDI) [22] is commonly used. The CTDI calculation is based on the measurements taken with a standardized cylindrical phantom [23] made of polymethyl methacrylate (PMMA). Measurements are taken at the center and at the periphery of the phantom using an ion chamber. The weighted sum of these measurements represents the dose absorbed by patients.

For nuclear medicine, the Medical Internal Radiation Dosimetry (MIRD) [24] is used to calculate the absorbed dose from radioisotopes. The method calculates the absorbed dose to neighboring organs per radioisotope decay in a source organ, called the S-factor, using Monte Carlo for each radioisotope. The absorbed dose is then calculated by multiplying the time-integrated radioactivity of radioisotopes and S-factors.

While both CTDI and MIRD provide simplified approaches to estimate absorbed dose to patients or internal organs, patient-specific factors, i.e., patient size, and patient anatomy, should be considered for personalized dose estimation. This is particularly crucial in theragnostic applications, which involve simultaneous imaging and treatment using radiopharmaceuticals [25]. In theragnostic applications, the employed dose level (~20 Gy) is significantly higher than that used for the imaging-only purposes (~10 mSv=0.01 Gy). Therefore, accurate dose calculation for both tumors and neighboring normal organs is of utmost importance to achieve clinical goals.

To improve precision of dose calculation, the convolution/superposition methods have been developed [26?29]. These methods model the dose deposition of external or internal radiation sources using point-spread-kernels [30?34] and estimate the dose distribution through convolution and superposition operations. The point-spread-kernels, which describe the contribution of dose deposition from a source, are obtained through MC simulation to estimate the dose contribution to all potential locations from a point source.

However, the convolution/superposition algorithms typically yield higher errors with heterogeneous media [35?38]. Higher precision in dose calculation can be achieved by estimating the dose with MC simulation without model-based approximations. Therefore, MC-based dose calculation has been investigated for chest radiography [39, 40], CT [41?43], breast CT [44, 45], PET [46?48], SPECT [49], and digital breast tomosynthesis (DBT) [50?52]. MC-based dosimetry methods showed good agreement with experimental measurements, typically within 4% [53, 54].

3.2 Image reconstruction and artifact correction

In volumetric reconstruction of medical imaging data, the system matrix is required to represent the contribution of detected signals in the image domain. The matrix maps data between image and detector domains, and its accuracy significantly impacts the image quality. MC can generate a high-quality system matrix that considers radiation physics, detector response, and particle characteristics for Tomographic Gamma Scanning [55], PET [56, 57], and SPECT [58, 59] image reconstruction.

MC methods also play a crucial role in artifact correction. Typically, image reconstruction and processing algorithms assume that the measured signals originate from mono-energetic particles and travel straight between the source and the detector. However, in reality, particles exhibit polychromatic energy distributions and can be scattered during travel due to interaction with imaging subjects. These discrepancies introduce imaging artifacts, such as scatter and beam hardening, which degrade image quality.

Scatter artifacts are common in medical imaging and significantly degrades image quality. Several scatter correction methods have been studied to remove scattered signals, including rejection methods that use a collimator or anti-scatter grid [60?62], beam-blocker-based estimation and removal methods [63?65], model-based methods [66, 67], and data-driven methods [68?70]. MC methods can also be used to correct for the scatter artifact by integrating MC simulation steps with image reconstruction frameworks to estimate and remove the scattered signals [71?74]. In such applications, fast MC methods are employed to minimize computational overhead.

Furthermore, MC methods can estimate the energy spectrum of the X-ray tube, which is necessary to account for the polychromatic nature of X-rays during image reconstruction [75]. They can also correct other imaging artifacts, including beam hardening, metal artifacts, partial volume effects, and off-focal radiation [76].

3.3 Virtual clinical trial

The virtual clinical trial (VCT) [77?79], also known as an *in-silico* clinical trial, is a computational approach used to estimate the effects of treatment and medical devices by modeling human anatomy, physiology, drugs, and medical devices. Unlike traditional clinical trials, which involve subject recruitment, data acquisition, efficacy evaluation, and safety evaluation, the VCTs are time-saving and cost-effective alternatives that requires less manpower to reach conclusions.

The VCTs have also been adapted for medical imaging devices [79]. In this framework, MC plays a pivotal role as it can accurately model the imaging devices, imaging subjects, and interactions between particles and materials. Therefore, MC has been used for VCTs to validate and characterize breast imaging systems [80?84], develop and validate image reconstruction algorithms [85?93], and investigate novel imaging systems [94?96], and detectors [97?99].

Recently, the VCTs have become increasingly important in the development of data-driven algorithms due to their need for large datasets. MC methods can produce artifact-free data or filter detected signals based on the origin of generation, interaction, and particle energy. This capability allows for the generation of input data that mimics experimental measurements and paired desired output, tailored to the objectives of the study. Consequently, MC simulations are commonly used to collect data for training deep neural networks that estimate scatter artifacts [68?70, 100, 101], solve inverse problems for image reconstruction [102, 103], reconstruct under-sampled data [104], denoise low-dose medical images [105], and estimate dose exposure from imaging [106, 107].

4 MC codes available for medical imaging research

There are several MC codes available for modeling medical imaging systems, each with its own advantages. This section covers available codes categorized into 4 groups: (1) general-purpose MC codes for experts, (2) user-friendly general-purpose codes, (3) GPU-based accelerated MC codes, and (4) commercial MC software packages.

4.1 Geant4/Electron Gamma Shower (EGS)/FLUKA

Geant4 [108], EGSnrc [109], and FLUKA [110] are widely used MC codes for radiation transport problems. These general-purpose codes support a wide range of particle interactions, geometric components, and scoring functions. They have a broad range of applications, including medical linear accelerators (LINACs) [111?115], charged particle accelerators [116?119], and medical imaging modalities such as CT [120?123], PET [124?127], SPECT [128, 129], prompt gamma [130, 131], proton imaging [132, 133], and mammography [134].

These MC codes offer extensive customizability, allowing users to add various features, including geometric components, scoring functions, and VRTs. However, setting up the simulation environment, running simulations, and adding new features require substantial programming and physics knowledge.

4.2 Geant4 Application for Tomographic Emission (GATE)/TOols for PArticle imulation (TOPAS))

GATE [135, 136] and TOPAS [14, 15] are general-purpose MC codes that serve as wrapper for Geant4. They support macro-based or text-based input parameters for setting up simulation environments without requiring programming knowledge. Additionally, they offer pre-built functions to facilitate simulations.

GATE is primarily designed for medical imaging device modeling, providing extensive scoring functions, geometric components, examples, and file formats commonly used in clinics, i.e., DICOM, MHA, and MHD. Numerous studies have utilized GATE to model various medical imaging systems, including CT/CBCT [93, 137?139], MVCT [20, 140?142], PET [137, 143?147], SPECT [137, 144, 147], prompt gamma [148, 149], and mammography [150].

TOPAS was initially designed to model proton beamlines and medical LINACs, and has recently expanded to include features for medical imaging devices through extensions [16, 151]. The TOPAS-imaging [16] extension supports detector geometries and scoring functions for CBCT, PET, SPECT, and prompt gamma imaging systems. The fastCAT [151] framework provides an integrated framework for CBCT imaging and reconstruction.

4.3 GPU geant4-based based Monte Carlo simulation (GGEMS)/MCGPU/MCPET

The aforementioned MC codes are general-purpose and support a wide range of particles and interactions, including electrons, photons, optical photons, and charged particles. This versatility allows them to model various imaging modalities regardless of the particles, interactions, or geometries. However, they are currently only implemented on computer processing units (CPUs), which necessitates extensive computational resources for simulations, creating a bottleneck. To mitigate this computational burden, multithreading and distributed computing approaches have been widely employed [152?155].

Recent advancement in graphic processing units (GPUs) and programming methods have further improve computational efficiency. GPU-based MC codes such as GGEMS [156], MCGPU [83, 157, 158], and MCGPU-PET [159] transport particles in parallel to improve the efficiency. GGEMS is used for modeling CBCT and SPECT systems. MCGPU aims to model CBCT and DBT systems, and MCGPU-PET aims to model PET systems.

These GPU-based codes focus on the photoelectric effect, Compton scattering, and Rayleigh scattering of photons, interactions that are most significant for CBCT, PET, SPECT, and DBT systems. They also support geometric components and scanning geometries commonly used in medical imaging modalities. However, modifications are needed to model modalities with atypical geometries, such as non-isocentric geometry in CBCT [160].

The results obtained from the GPU-accelerated MC codes demonstrated excellent agreement with general-purpose MC codes, such as GATE [135] and PENELOPE [161, 162], with discrepancies below 1% for CBCT applications and

below 10% for PET applications. Notably, the GPU-accelerated MC codes required approximately 100 times less computation time compared to the general-purpose MC codes.

4.4 Commercial software packages

Commercial software packages supporting MC-based dose calculation for nuclear medicine, include Torch (Voximetry, Madison, WI, USA) [163] and Voxel Dosimetry (Hermes Medical Solutions, Stockholm, Sweden) [164]. These packages employ GPU-accelerated MC [165] or semi-MC [166] to calculate internal organ dose from SPECT/CT or PET/CT images within a timeframe suitable for clinical practice.

5 Potential research areas

5.1 Virtual human phantom and 4D simulation

Most studies in the VCT framework currently utilize existing patient or phantoms images to reproduce raw imaging data. The diversity of the imaging data can be further enhanced by adopting virtual phantoms that closely resemble human anatomy. Extensive studies have been conducted to develop such phantoms, including XCAT phantoms [167], NCI phantoms [168, 169], and breast phantoms [170, 171]. These phantoms account for a variety of human anatomies and include breathing and cardiac motion for realistic simulation.

Further investigation is needed to obtain more diverse and realistic images using virtual phantoms that incorporate vasculature networks, blood flow, synthetic lesions, and synthetic implants. This approach will alleviate the experimental burden in research projects and facilitate the exploration of novel methods for vascular imaging devices and 4D imaging techniques. Additionally, it can aid in the development and validation of data-driven methods by providing data that closely resembles human anatomy and disease, thereby improving the reliability of data-driven smethods.

5.2 Benchmarking and validation datasets

Several MC codes are available for imaging research, with ongoing development to meet the specific requirements of individual research project. The physics models and results of these new MC codes have been independently validated. However, an extensive comparison between different codes has not yet been conducted. Such a comparison is important for identifying the limitations and advantages of each code and will provide essential information for researchers to choose the most appropriate MC code for their study.

A study conducted by an American Association of Physicists in Medicine (AAPM) Task Group provided detailed description of the simulation setup and datasets used to compare the half-value layer, dose exposure, and fluence of CT, radiography, and tomosynthesis systems [172]. This study also compared the results of different general-purpose MC codes. Further investigations are required to cover various imaging modalities, such as PET, SPECT, spectral CT, and MVCT, and to conduct experimental validation. Additionally, it would be desirable to establish testing criteria to compare computational costs, as was done for MC-based dose calculation comparisons [173], since most recently developed MC codes utilize advanced computational techniques and hardware to minimize computational cost.

5.3 Deterministic solver

Although MC methods provide accurate modeling for imaging modalities, they require extensive computational resources. Consequently, numerous studies have been conducted to minimize computational costs using parallelization methods and variance reduction techniques, as previously discussed. Another approach to reducing the computational cost is to solve the LBTE deterministically.

The deterministic solution can be obtained by discretizing variables (energy, angle, and space) and employing numerical methods [174]. The deterministic approaches converge to the same solution obtained by MC codes. The uncertainty of the deterministic solution depends on the granularity of variable discretization, whereas in MC methods, it depends on the number of particles tracked.

Research into deterministic solvers has been applied to estimate scattered X-ray signals and correct them in CT images [175?177], as well as to estimate patient dose exposure during CT imaging [178?180]. While deterministic approaches have demonstrated equivalent results to MC methods [176, 180], they remain unexplored compared to MC methods. Comprehensive investigations are required to extend the deterministic solvers to other imaging modalities such as PET, SPECT, thereby enhancing their application in medical imaging research.

Author contributions Hoyeon Lee conceptualized the review, performed literature search, and wrote the manuscript.

Funding Nothing to disclose.

Declarations

Conflict of interest Nothing to disclose.

Ethical approval This work does not contain any human or animal subjects.

Consent to participate There are no human participants in these studies.

Consent to publish There are no human participants in these studies.

References

1. Laal M. Innovation process in medical imaging. Proc Soc Behav Sci. 2013;81:60?4. https://doi.org/10.1016/j.sbspro.2013.06.388.
2. Hussain S, Mubeen I, Ullah N, Shah SSUD, Khan BA, Zahoor M, et al. Modern diagnostic imaging technique applications and risk factors in the medical field: a review. BioMed Res Int. 2022;2022:5164970. https://doi.org/10.1155/2022/5164970.
3. Morin O, Gillis A, Chen J, Aubin M, Bucci MK, Roach M, et al. Megavoltage cone-beam CT: system description and clinical applications. Med Dosim. 2006;31:51?61. https://doi.org/10.1016/j.meddos.2005.12.009.
4. Srinivasan K, Mohammadi M, Shepherd J. Applications of linac-mounted kilovoltage cone-beam computed tomography in modern radiation therapy: a review. Pol J Radiol. 2014;79:181?93.
5. Shakirin G, Braess H, Fiedler F, Kunath D, Laube K, Parodi K, et al. Implementation and workflow for PET monitoring of therapeutic ion irradiation: a comparison of in-beam, in-room, and off-line techniques. Phys Med Biol. 2011;56:1281?98. https://doi.org/10.1088/0031-9155/56/5/004.
6. Krimmer J, Dauvergne D, Létang JM, Testa É. Prompt-gamma monitoring in hadrontherapy: a review. Nucl Instrum Methods Phys Res Sect A: Accel Spectrometers Detect Assoc Equip. 2018;878:58?73. https://doi.org/10.1016/j.nima.2017.07.063.
7. Sale KE, JrPM B, Buck RM, Cullen D, Fujino D, Hartmann-Siantar C. Applications of the Monte Carlo radiation transport toolkit at LLNL. Radiat Sources Radiat Interact. 1999. https://doi.org/10.1117/12363708.
8. Razani A. A Monte Carlo method for radiation transport calculations. J Nucl Sci Technol. 1972;9:551?4. https://doi.org/10.3327/jnst.9.551.
9. Vassiliev ON. Monte Carlo methods for radiation transport, fundamentals and advanced topics. Biol Med Phys Biomed Eng. 2016. https://doi.org/10.1007/978-3-319-44141-2_7.
10. Stanley DN, Papanikolaou N, Gutiérrez AN. An evaluation of the stability of image-quality parameters of varian on-board imaging (OBI) and EPID imaging systems. J Appl Clin Méd Phys. 2015;16:87?98. https://doi.org/10.1120/jacmp.v16i2.5088.
11. Gach HM, Tanase C, Boada F. (2008) 2D & 3D Shepp-Logan Phantom Standards for MRI. In: 2008 19th Int Conf Syst Eng 521?6. https://doi.org/10.1109/icseng.2008.15.
12. Pan T, Einstein SA, Kappadath SC, Grogg KS, Gomez CL, Alessio AM, et al. Performance evaluation of the 5-ring GE Discovery MI PET/CT system using the national electrical manufacturers association NU 2?2012 Standard. Méd Phys. 2019;46:3025?33. https://doi.org/10.1002/mp.13576.
13. MacFarlane CR. Radiologists AC of. ACR accreditation of nuclear medicine and PET imaging departments. J Nucl Med Technol. 2006;34:18?24.
14. Perl J, Shin J, Schümann J, Faddegon B, Paganetti H. TOPAS: an innovative proton Monte Carlo platform for research and clinical applications. Med Phys. 2012;39:6818?37. https://doi.org/10.1118/1.4758060.
15. Faddegon B, Ramos-Méndez J, Schuemann J, McNamara A, Shin J, Perl J, et al. The TOPAS tool for particle simulation, a Monte Carlo simulation tool for physics, biology and clinical research. Phys Medica. 2020;72:114?21. https://doi.org/10.1016/j.ejmp.2020.03.019.
16. Lee H, Cheon B-W, Feld JW, Grogg K, Perl J, Ramos-Méndez JA, et al. TOPAS-imaging: extensions to the TOPAS simulation toolkit for medical imaging systems. Phys Med Biol. 2023;68:084001. https://doi.org/10.1088/1361-6560/acc565.
17. Mainegra-Hing E, Kawrakow I. Variance reduction techniques for fast Monte Carlo CBCT scatter correction calculations. Phys Med Biol. 2010;55:4495?507. https://doi.org/10.1088/0031-9155/55/16/s05.
18. Staelens S, Beenhouwer JD, Kruecker D, Maigne L, Rannou F, Ferrer L, et al. GATE: Improving the computational efficiency. Nucl Instrum Methods Phys Res Sect A: Accel Spectrometers, Detect Assoc Equip. 2006;569:341?5. https://doi.org/10.1016/j.nima.2006.08.070.
19. Haynor DR, Harrison RL, Lewellen TK, Bice AN, Anson CP, Gillispie SB, et al. Improving the efficiency of emission tomography simulations using variance reduction techniques. IEEE Trans Nucl Sci. 1990;37:749?53. https://doi.org/10.1109/23.106709.
20. Shi M, Myronakis M, Hu Y-H, Jacobson M, Lehmann M, Fueglistaller R, et al. A novel method for fast image simulation of flat panel detectors. Phys Med Biology. 2019;64:095019. https://doi.org/10.1088/1361-6560/ab12aa.
21. Lin EC. Radiation risk from medical imaging. Mayo Clin Proc. 2010;85:1142?6. https://doi.org/10.4065/mcp.2010.0260.
22. Shope TB, Gagne RM, Johnson GC. A method for describing the doses delivered by transmission X-ray computed tomography. Med Phys. 1981;8:488?95. https://doi.org/10.1118/1.594995.
23. Treb K, Li K. Accuracy of weighted CTDI in estimating average dose delivered to CTDI phantoms: an experimental study. Méd Phys. 2020;47:6484?99. https://doi.org/10.1002/mp.14528.
24. Toohey RE, Stabin MG, Watson EE. The AAPM/RSNA physics tutorial for residents. Radiographics. 2000;20:533?46. https://doi.org/10.1148/radiographics.20.2.g00mc33533.
25. Marin JFG, Nunes RF, Coutinho AM, Zaniboni EC, Costa LB, Barbosa FG, et al. Theranostics in nuclear medicine: emerging and re-emerging integrated imaging and therapies in the era of precision oncology. Radiographics. 2020;40:1715?40. https://doi.org/10.1148/rg.2020200021.
26. Reinhart AM, Fast MF, Ziegenhein P, Nill S, Oelfke U. A kernel-based dose calculation algorithm for kV photon beams with explicit handling of energy and material dependencies. Br J Radiol. 2016;90:20160426. https://doi.org/10.1259/bjr.20160426.
27. Heidarloo N, Aghamiri SMR, Saghamanesh S, Azma Z, Alaei P. A novel analytical method for computing dose from kilovoltage beams used in image-guided radiation therapy. Phys Med. 2022;96:54?61. https://doi.org/10.1016/j.ejmp.2022.02.020.
28. Graves S, Tiwari A, Sunderland J. Collapsed-cone convolution superposition for improved accuracy of voxelwise dosimetry. J Nucl Med. 2020;61:535.
29. Tian X, Segars WP, Dixon RL, Samei E. Convolution-based estimation of organ dose in tube current modulated CT. Phys Med Biol. 2016;61:3935?54. https://doi.org/10.1088/0031-9155/61/10/3935.
30. Graves SA, Flynn RT, Hyer DE. Dose point kernels for 2,174 radionuclides. Med Phys. 2019;46:5284?93. https://doi.org/10.1002/mp.13789.

31. Heidarloo N, Aghamiri SMR, Saghamanesh S, Azma Z, Alaei P. Generation of material-specific energy deposition kernels for kilovoltage X-ray dose calculations. Med Phys. 2021. https://doi.org/10.1002/mp.15061.
32. Alaei P, Gerbi BJ, Geise RA. Generation and use of photon energy deposition kernels for diagnostic quality X rays. Med Phys. 1999;26:1687?97. https://doi.org/10.1118/1.598674.
33. Tiwari A, Graves S, Sunderland J. Measurements of dose point kernels using GATE Monte Carlo toolkit for personalized convolution dosimetry. J Nucl Med. 2019;60:274.
34. Papadimitroulas P. Dosimetry applications in GATE Monte Carlo toolkit. Phys Med. 2017;41:136?40. https://doi.org/10.1016/j.ejmp.2017.02.005.
35. Huang C-Y, Chu T-C, Lin S-Y, Lin J-P, Hsieh C-Y. Accuracy of the convolution/superposition dose calculation algorithm at the condition of electron disequilibrium. Appl Radiat Isot. 2002;57:825?30. https://doi.org/10.1016/s0969-8043(02)00228-2.
36. Jacques R, McNutt T. An improved method of heterogeneity compensation for the convolution/superposition algorithm. J Phys Conf Ser. 2014;489:012019. https://doi.org/10.1088/1742-6596/489/1/012019.
37. Aspradakis MM, Morrison RH, Richmond ND, Steele A. Experimental verification of convolution/superposition photon dose calculations for radiotherapy treatment planning. Phys Med Biol. 2003;48:2873?93. https://doi.org/10.1088/0031-9155/48/17/309.
38. Bertolet A, Wehrenberg-Klee E, Bobi? M, Grassberger C, Perl J, Paganetti H, et al. Pre- and post-treatment image-based dosimetry in 90Y-microsphere radioembolization using the TOPAS Monte Carlo toolkit. Phys Med Biol. 2021. https://doi.org/10.1088/1361-6560/ac43fd.
39. Koblinger L, Zarand P. Monte Carlo calculations on chest X-ray examinations for the determination of the absorbed dose and image quality. Phys Med Biol. 1973;18:518?31. https://doi.org/10.1088/0031-9155/18/4/004.
40. Correa SCA, Souza EM, Silva AX, Lopes RT, Yoriyaz H. Dose?image quality study in digital chest radiography using Monte Carlo simulation. Appl Radiat Isot. 2008;66:1213?7. https://doi.org/10.1016/j.apradiso.2008.01.009.
41. Salvadó M, López M, Morant JJ, Calzado A. Monte Carlo calculation of radiation dose in CT examinations using phantom and patient tomographic models. Radiat Prot Dosim. 2005;114:364?8. https://doi.org/10.1093/rpd/nch516.
42. Jia X, Yan H, Gu X, Jiang SB. Fast Monte Carlo simulation for patient-specific CT/CBCT imaging dose calculation. Phys Med Biol. 2012;57:577?90. https://doi.org/10.1088/0031-9155/57/3/577.
43. Sharma S, Kapadia A, Fu W, Abadi E, Segars WP, Samei E. A real-time Monte Carlo tool for individualized dose estimations in clinical CT. Phys Med Biol. 2019;64:215020. https://doi.org/10.1088/1361-6560/ab467f.
44. Shim S, Kolditz D, Steiding C, Ruth V, Hoetker AM, Unkelbach J, et al. Radiation dose estimates based on Monte Carlo simulation for spiral breast computed tomography imaging in a large cohort of patients. Med Phys. 2023;50:2417?28. https://doi.org/10.1002/mp.16211.
45. Sarno A, Mettivier G, Tucciariello RM, Bliznakova K, Boone JM, Sechopoulos I, et al. Monte Carlo evaluation of glandular dose in cone-beam X-ray computed tomography dedicated to the breast: homogeneous and heterogeneous breast models. Phys Med. 2018;51:99?107. https://doi.org/10.1016/j.ejmp.2018.05.021.
46. Peng Z, Lu Y, Xu Y, Li Y, Cheng B, Ni M, et al. Development of a GPU-accelerated Monte Carlo dose calculation module for nuclear medicine ARCHER-NM: demonstration for a PET/CT imaging procedure. Phys Med Biol. 2022. https://doi.org/10.1088/1361-6560/ac58dd.
47. Neira S, Guiu-Souto J, Díaz-Botana P, Pais P, Fernández C, Pubul V, et al. Quantification of internal dosimetry in PET patients: individualized Monte Carlo vs generic phantom-based calculations. Med Phys. 2020;47:4574?88. https://doi.org/10.1002/mp.14344.
48. Neira S, Guiu-Souto J, Pais P, de Llano SRM, Fernández C, Pubul V, et al. Quantification of internal dosimetry in PET patients II: individualized Monte Carlo-based dosimetry for [18F] fluorocholine PET. Med Phys. 2021;48:5448?58. https://doi.org/10.1002/mp.15090.
49. Momennezhad M, Nasseri S, Zakavi S, Parach A, Ghorbani M, Asl R. A 3D Monte Carlo method for estimation of patient-specific internal organs absorbed dose for 99m Tc-hynic-Tyr 3 -octreotide imaging. World J Nucl Med. 2016;15:114?23. https://doi.org/10.4103/1450-1147.174700.
50. Rodrigues L, Magalhaes LAG, Braz D. Monte Carlo simulation for the estimation of the glandular breast dose for a digital breast tomosynthesis system. Radiat Prot Dosim. 2014;167:576?83. https://doi.org/10.1093/rpd/ncu352.
51. Baptista M, Maria SD, Oliveira N, Matela N, Janeiro L, Almeida P, et al. Image quality and dose assessment in digital breast tomosynthesis: a Monte Carlo study. Radiat Phys Chem. 2014;104:158?62. https://doi.org/10.1016/j.radphyschem.2013.12.036.
52. Massera RT, Tomal A, Thomson RM. Multiscale Monte Carlo simulations for dosimetry in X-ray breast imaging: part I?macroscopic scales. Med Phys. 2023. https://doi.org/10.1002/mp.16910.
53. Wang L, Lovelock M, Chui C. Experimental verification of a CT-based Monte Carlo dose-calculation method in heterogeneous phantoms. Med Phys. 1999;26:2626?34. https://doi.org/10.1118/1.598802.
54. Van B, Dewaraja YK, Niedbala JT, Rosebush G, Kazmierski M, Hubers D, et al. Experimental validation of Monte Carlo dosimetry for therapeutic beta emitters with radiochromic film in a 3D-printed phantom. Med Phys. 2023;50:540?56. https://doi.org/10.1002/mp.15926.
55. Agarwal C, Mhatre A, Patra S, Chaudhury S, Goswami A. Algebraic reconstruction technique combined with Monte Carlo method for weight matrix calculation in gamma ray transmission tomography. SN Appl Sci. 2019;1:1157. https://doi.org/10.1007/s42452-019-1201-1.
56. Zhang L, Staelens S, Holen RV, Beenhouwer JD, Verhaeghe J, Kawrakow I, et al. Fast and memory-efficient Monte Carlo-based image reconstruction for whole-body PET. Med Phys. 2010;37:3667?76. https://doi.org/10.1118/1.3455287.
57. Saha K, Straus KJ, Chen Yu, Glick SJ. Iterative reconstruction using a Monte Carlo based system transfer matrix for dedicated breast positron emission tomography. J Appl Phys. 2014;116:084903. https://doi.org/10.1063/1.4894085.
58. Nguyen MP, Goorden MC, Ramakers RM, Beekman FJ. Efficient monte-carlo based system modelling for image reconstruction in preclinical pinhole SPECT. Phys Med Biol. 2021;66:125013. https://doi.org/10.1088/1361-6560/ac0682.
59. Peterson M, Gustafsson J, Ljungberg M. Monte Carlo-based quantitative pinhole SPECT reconstruction using a ray-tracing back-projector. EJNMMI Phys. 2017;4:32. https://doi.org/10.1186/s40658-017-0198-z.
60. Stankovic U, Ploeger LS, van Herk M, Sonke J. Optimal combination of anti-scatter grids and software correction for CBCT imaging. Med Phys. 2017;44:4437?51. https://doi.org/10.1002/mp.12385.
61. Yu Z, Park Y, Altunbas C. (2020) Simultaneous scatter rejection and correction method using 2D antiscatter grids for

CBCT. Med Imaging 2020: Phys Med Imaging. 11312: 104 https://doi.org/10.1117/12.2549763.
62. Cho S, Lim S, Kim C, Wi S, Kwon T, Youn WS, et al. Enhancement of soft-tissue contrast in cone-beam CT using an anti-scatter grid with a sparse sampling approach. Phys Med. 2020;70:1?9. https://doi.org/10.1016/j.ejmp.2020.01.004.
63. Sakaltras N, Pena A, Martinez C, Desco M, Abella M. A novel beam stopper-based approach for scatter correction in digital planar radiography. Sci Rep. 2023;13:8795. https://doi.org/10.1038/s41598-023-32764-5.
64. Létang JM, Babot D. A beam stop based correction procedure for high spatial frequency scatter in industrial cone-beam X-ray CT. Nuclear instruments and methods in physics research section B: Beam interactions with materials and atoms. 2008.
65. Lee H, Min J, Lee T, Pua R, Sabir S, Yoon K-H, et al. Investigation on beam-blocker-based scatter correction method for improving ct number accuracy. IEEE T Nucl Sci. 2017;64:908?14. https://doi.org/10.1109/tns.2017.2669519.
66. Wang A, Shapiro E, Yoon S, Ganguly A, Proano C, Colbeth R, et al. Asymmetric scatter kernels for software-based scatter correction of gridless mammography. Proc Spie. 2015. https://doi.org/10.1117/122081501.
67. Sun M, Star-Lack JM. Improved scatter correction using adaptive scatter kernel superposition. Phys Med Biol. 2010;55:6695?720. https://doi.org/10.1088/0031-9155/55/22/007.
68. Lalonde A, Winey B, Verburg J, Paganetti H, Sharp GC. Evaluation of CBCT scatter correction using deep convolutional neural networks for head and neck adaptive proton therapy. Phys Med Biol. 2020;65:245022. https://doi.org/10.1088/1361-6560/ab9fcb.
69. Maier J, Sawall S, Knaup M, Kachelrieß M. Deep scatter estimation (DSE): accurate real-time scatter estimation for X-ray CT using a deep convolutional neural network. J Nondestruct Eval. 2018;37:57. https://doi.org/10.1007/s10921-018-0507-z.
70. Maier J, Eulig E, Vöth T, Knaup M, Kuntz J, Sawall S, et al. Real-time scatter estimation for medical CT using the deep scatter estimation: method and robustness analysis with respect to different anatomies, dose levels, tube voltages, and data truncation. Med Phys. 2019;46:238?49. https://doi.org/10.1002/mp.13274.
71. Kim K, Lee T, Seong Y, Lee J, Jang KE, Choi J, et al. Fully iterative scatter corrected digital breast tomosynthesis using GPU-based fast Monte Carlo simulation and composition ratio update. Med Phys. 2015;42:5342?55. https://doi.org/10.1118/1.4928139.
72. Bayerlein R, Spencer BA, Leung EK, Omidvari N, Abdelhafez YG, Wang Q, et al. Development of a Monte Carlo-based scatter correction method for total-body PET using the uEXPLORER PET/CT scanner. Phys Med Biol. 2024;69:045033. https://doi.org/10.1088/1361-6560/ad2230.
73. Moore SC, Ouyang J, Park M-A, Fakhri GE. Monte Carlo-based compensation for patient scatter, detector scatter, and crosstalk contamination in In-111 SPECT imaging. Nucl Instrum Methods Phys Res Sect A: Accel, Spectrometers, Detect Assoc Equip. 2006;569:472?6. https://doi.org/10.1016/j.nima.2006.08.079.
74. Alsaffar A, Kieß S, Sun K, Simon S. Computational scatter correction in near real-time with a fast Monte Carlo photon transport model for high-resolution flat-panel CT. J Real-time Image Pr. 2022. https://doi.org/10.1007/s11554-022-01247-7.
75. Nazemi E, Six N, Iuso D, Samber BD, Sijbers J, Beenhouwer JD. monte-carlo-based estimation of the X-ray energy spectrum for CT artifact reduction. Appl Sci. 2021;11:3145. https://doi.org/10.3390/app11073145.
76. Maier J, Leinweber C, Sawall S, Stoschus H, Ballach F, Müller T, et al. Simulation-based artifact correction (SBAC) for metrological computed tomography. Meas Sci Technol. 2017;28:065011. https://doi.org/10.1088/1361-6501/aa666e.
77. Pappalardo F, Russo G, Tshinanu FM, Viceconti M. In silico clinical trials: concepts and early adoptions. Brief Bioinform. 2019;20:1699?708. https://doi.org/10.1093/bib/bby043.
78. Badano A. In silico imaging clinical trials: cheaper, faster, better, safer, and more scalable. Trials. 2021;22:64. https://doi.org/10.1186/s13063-020-05002-w.
79. Abadi E, Segars WP, Tsui BMW, Kinahan PE, Bottenus N, Frangi AF, et al. Virtual clinical trials in medical imaging: a review. J Med Imaging. 2020;7:042805?042805. https://doi.org/10.1117/1.jmi.7.4.042805.
80. di Franco F, Sarno A, Mettivier G, Hernandez AM, Bliznakova K, Boone JM, et al. GEANT4 Monte Carlo simulations for virtual clinical trials in breast X-ray imaging: proof of concept. Phys Med. 2020;74:133?42. https://doi.org/10.1016/j.ejmp.2020.05.007.
81. Mettivier G, Sarno A, Lai Y, Golosio B, Fanti V, Italiano ME, et al. Virtual clinical trials in 2D and 3D X-ray breast imaging and dosimetry: comparison of CPU-based and GPU-based Monte Carlo codes. Cancers. 2022;14:1027. https://doi.org/10.3390/cancers14041027.
82. Badano A, Graff CG, Badal A, Sharma D, Zeng R, Samuelson FW, et al. Evaluation of digital breast tomosynthesis as replacement of full-field digital mammography using an in silico imaging trial. Jama Netw Open. 2018;1:185474. https://doi.org/10.1001/jamanetworkopen.2018.5474.
83. Badal A, Sharma D, Graff CG, Zeng R, Badano A. Mammography and breast tomosynthesis simulator for virtual clinical trials. Comput Phys Commun. 2021;261:107779. https://doi.org/10.1016/j.cpc.2020.107779.
84. Sarno A, Mettivier G, Franco F di, Paternò G, Taibi A, Cardarelli P et al. (2020) Advanced Monte Carlo application for in-silico clinical trials in x-ray breast imaging. In: 15th Int Work Breast Imaging (IWBI2020). https://doi.org/10.1117/12.2563322.
85. Efthimiou N, Emond E, Wadhwa P, Cawthorne C, Tsoumpas C, Thielemans K. Implementation and validation of time-of-flight PET image reconstruction module for listmode and sinogram projection data in the STIR library. Phys Med Biol. 2019;64:035004. https://doi.org/10.1088/1361-6560/aaf9b9.
86. Holen RV, Vandenberghe S, Staelens S, Beenhouwer JD, Lemahieu I. Fast 3D iterative image reconstruction for SPECT with rotating slat collimators. Phys Med Biol. 2009;54:715?29. https://doi.org/10.1088/0031-9155/54/3/016.
87. Karpetas GE, Michail CM, Fountos GP, Valais IG, Nikolopoulos D, Kandarakis IS, et al. Influence of iterative reconstruction algorithms on PET image resolution. J Phys Conf Ser. 2015;637:012011. https://doi.org/10.1088/1742-6596/637/1/012011.
88. Krzemien W, Gajos A, Kacprzak K, Rakoczy K, Korcyl G. J-PET framework: software platform for PET tomography data reconstruction and analysis. SoftwareX. 2020;11:100487. https://doi.org/10.1016/j.softx.2020.100487.
89. Toussaint M, Lecomte R, Dussault J-P. Improvement of spatial resolution with iterative PET reconstruction using ultrafast TOF. IEEE Trans Radiat Plasma Med Sci. 2021;5:729?37. https://doi.org/10.1109/trpms.2020.3033561.
90. Zhang H, Wang Y, Qi J, Abbaszadeh S. Penalized maximum-likelihood reconstruction for improving limited-angle artifacts in a dedicated head and neck PET system. Phys Med Biol. 2020;65:165016?165016. https://doi.org/10.1088/1361-6560/ab8c92.
91. Yu X, Wang C, Hu H, Liu H. Low dose PET image reconstruction with total variation using alternating direction method. PLoS

ONE. 2016;11:0166871. https://doi.org/10.1371/journal.pone.0166871.
92. Zhang Z, Ye J, Chen B, Perkins AE, Rose S, Sidky EY, et al. Investigation of optimization-based reconstruction with an image-total-variation constraint in PET. Phys Med Biol. 2016;61:6055?84. https://doi.org/10.1088/0031-9155/61/16/6055.
93. Lee S, Choi Y-N, Kim H-J. A simulation study of high-resolution X-ray computed tomography imaging using irregular sampling with a photon-counting detector. Nucl Instrum Methods Phys Res Sect A: Accel, Spectrometers, Detect Assoc Equip. 2013;726:175?80. https://doi.org/10.1016/j.nima.2013.05.044.
94. Liu R, Zhang S, Zhao T, O?Sullivan JA, Williamson JF, Webb T, et al. Impact of bowtie filter and detector collimation on multislice CT scatter profiles: a simulation study. Med Phys. 2021;48:852?70. https://doi.org/10.1002/mp.14652.
95. Zeraatkar N, Farahani MH, Rahmim A, Sarkar S, Ay MR. Design and assessment of a novel SPECT system for desktop open-gantry imaging of small animals: a simulation study. Med Phys. 2016;43:2581?97. https://doi.org/10.1118/1.4947127.
96. Dedes G, Dickmann J, Giacometti V, Rit S, Krah N, Meyer S, et al. The role of Monte Carlo simulation in understanding the performance of proton computed tomography. Z für Med Phys. 2022;32:23?38. https://doi.org/10.1016/j.zemedi.2020.06.006.
97. O?Connell J, Kundu S, Saidaminov M, Bazalova-Carter M. Next generation high resolution perovskite direct conversion detector: Monte Carlo design optimisation and virtual clinical trial. Phys Med Biol. 2023;68:025016. https://doi.org/10.1088/1361-6560/acae15.
98. Roth D, Larsson E, Ljungberg M, Gleisner KS. Monte Carlo modelling of a compact CZT-based gamma camera with application to 177Lu imaging. EJNMMI Phys. 2022;9:35. https://doi.org/10.1186/s40658-022-00463-1.
99. Ozoemelam I, Myronakis M, Harris TC, Arroyo PC, Huber P, Jacobson MW, et al. Monte Carlo model of a prototype flat-panel detector for multi-energy applications in radiotherapy. Med Phys. 2023;50:5944?55. https://doi.org/10.1002/mp.16689.
100. Duan X, Sahu P, Huang H, Zhao W. Deep-learning convolutional neural network-based scatter correction for contrast enhanced digital breast tomosynthesis in both cranio-caudal and mediolateral-oblique views. J Med Imaging. 2023;10:S22404?S22404. https://doi.org/10.1117/1.jmi.10.s2.s22404.
101. Zhuo X, Lu Y, Hua Y, Liu H, Zhang Y, Hao S, et al. Scatter correction for cone-beam CT via scatter kernel superposition-inspired convolutional neural network. Phys Med Biol. 2023;68:075011. https://doi.org/10.1088/1361-6560/acbe8f.
102. Häggström I, Schmidtlein CR, Campanella G, Fuchs TJ. DeepPET: a deep encoder?decoder network for directly solving the PET image reconstruction inverse problem. Med Image Anal. 2019;54:253?62. https://doi.org/10.1016/j.media.2019.03.013.
103. Cui J, Liu X, Wang Y, Liu H. Deep reconstruction model for dynamic PET images. PLoS ONE. 2017;12:0184667. https://doi.org/10.1371/journal.pone.0184667.
104. Kim H, Lee H, Lee S, Choi Y-W, Choi YJ, Kim KH et al. (2022) A feasibility study of dual-energy digital breast tomosynthesis for three-compartment-breast imaging. Medical Imaging 2022 Phys Medical Imaging https://doi.org/10.1117/12.2611606
105. Eckert D, Wicklein J, Herbst M, Dwars S, Ritschl L, Kappler S, et al. Deep learning based tomosynthesis denoising: a bias investigation across different breast types. J Med Imaging. 2023;10:064003?064003. https://doi.org/10.1117/1.jmi.10.6.064003.
106. Lee MS, Hwang D, Kim JH, Lee JS. Deep-dose: a voxel dose estimation method using deep convolutional neural network for personalized internal dosimetry. Sci Rep. 2019;9:10308. https://doi.org/10.1038/s41598-019-46620-y.
107. Kim KM, Lee MS, Suh MS, Cheon GJ, Lee JS. Voxel-based internal dosimetry for 177Lu-labeled radiopharmaceutical therapy using deep residual learning. Nucl Med Mol Imaging. 2023;57:94?102. https://doi.org/10.1007/s13139-022-00769-z.
108. Agostinelli S, Allison J, Amako K, Apostolakis J, Araujo H, Arce P, et al. Geant4?a simulation toolkit. Nucl Instruments Methods Phys Res Sect Accel Spectrometers Detect Assoc Equip. 2003;506:250?303. https://doi.org/10.1016/s0168-9002(03)01368-8.
109. Standards NRC of CanadaMRCentreIR, ionisant C national de recherches du CanadaC de recherche en métrologie. É de rayonnement. EGSnrc?: logiciel pour la simulation Monte Carlo du rayonnement ionisant. 2021. Available from: https://github.com/nrc-cnrc/EGSnrc
110. Böhlen TT, Cerutti F, Chin MPW, Fassò A, Ferrari A, Ortega PG, et al. The FLUKA code: developments and challenges for high energy and medical applications. Nucl Data Sheets. 2014;120:211?4. https://doi.org/10.1016/j.nds.2014.07.049.
111. Pilicer E, Alpat B, Menichelli M, Servoli L, Tucceri P, Italiani M et al. (2011) Full Geant4 and FLUKA simulations of an e-LINAC for its use in particle detectors performance tests. In: 2011 12th Eur Conf Radiat Eff Compon Syst https://doi.org/10.1109/radecs.2011.6131366.
112. Haneefa KA, Cyriac TS, Musthafa MM, Raman RG, Hridya VT, Siddhartha A, et al. FLUKA Monte Carlo for basic dosimetric studies of dual energy medical linear accelerator. J Radiother. 2014;2014:1?7. https://doi.org/10.1155/2014/343979.
113. Patil AJ, Chavan ST, Krishnan R, Pethe SN, Bhoraskar VN, Dhole SD et al. Collimator Design of 15 MeV Linear Accelerator Based Thermal Neutron Source for Radiography. ["Satogata, Brown Todd and, Kevin"], editors. Conf Proc C. 2011;110328:2154?6.
114. Constantin M, Perl J, LoSasso T, Salop A, Whittum D, Narula A, et al. Modeling the Truebeam linac using a CAD to Geant4 geometry implementation: dose and IAEA-compliant phase space calculations. Med Phys. 2011;38:4018?24. https://doi.org/10.1118/1.3598439.
115. Vagena E, Stoulos S, Manolopoulou M. Geant4 simulations on medical Linac operation at 18MV: experimental validation based on activation foils. Radiat Phys Chem. 2016;120:89?97. https://doi.org/10.1016/j.radphyschem.2015.11.030.
116. Koz?owska WS, Böhlen TT, Cuccagna C, Ferrari A, Fracchiolla F, Magro G, et al. FLUKA particle therapy tool for Monte Carlo independent calculation of scanned proton and carbon ion beam therapy. Phys Med Biol. 2019;64:075012. https://doi.org/10.1088/1361-6560/ab02cb.
117. Battistoni G, Bauer J, Boehlen TT, Cerutti F, Chin MPW, Augusto RDS, et al. The FLUKA Code: an accurate simulation tool for particle therapy. Front Oncol. 2016;6:116. https://doi.org/10.3389/fonc.2016.00116.
118. Jiang H, Paganetti H. Adaptation of GEANT4 to Monte Carlo dose calculations based on CT data. Med Phys. 2004;31:2811?8. https://doi.org/10.1118/1.1796952.
119. Hamad MKh. Bragg-curve simulation of carbon-ion beams for particle-therapy applications: a study with the GEANT4 toolkit. Nucl Eng Technol. 2021;53:2767?73. https://doi.org/10.1016/j.net.2021.02.011.
120. Somasundaram E, Artz NS, Brady SL. Development and validation of an open source Monte Carlo dosimetry model for wide-beam CT scanners using Fluka. J Appl Clin Med Phys. 2019;20:132?47. https://doi.org/10.1002/acm2.12559.
121. Spezi E, Downes P, Radu E, Jarvis R. Monte Carlo simulation of an X-ray volume imaging cone beam CT unit. Med Phys. 2009;36:127?36. https://doi.org/10.1118/1.3031113.
122. Brochu FM, Burnet NG, Jena R, Plaistow R, Parker MA, Thomas SJ. Geant4 simulation of the Elekta XVI kV CBCT unit for

accurate description of potential late toxicity effects of image-guided radiotherapy. Phys Med Biol. 2014;59:7601?8. https://doi.org/10.1088/0031-9155/59/24/7601.
123. Zou J, Hu Z, Gui J, Rong J, Li Y, Zheng H. (2010) Geant4-Based Monte Carlo Simulator for Fan-and Cone-Beam X-ray CT. In: 2010 4th Int Conf Bioinform Biomed Eng. https://doi.org/10.1109/icbbe.2010.5514746.
124. Augusto RS, Bauer J, Bouhali O, Cuccagna C, Gianoli C, Koz?owska WS, et al. An overview of recent developments in FLUKA PET tools. Phys Med. 2018;54:189?99. https://doi.org/10.1016/j.ejmp.2018.06.636.
125. Nasirzadeh Y, Ghal-Eh N, Yazdi MHH. Modeling GE advance PET-scanner using FLUKA simulation code. Appl Radiat Isot. 2022;184:110211. https://doi.org/10.1016/j.apradiso.2022.110211.
126. Fiedler K, Frach T, Rütten W, Solf T, Thon A. (2003) Assessment of the spatial resolution of PET scanners using a Geant4-based Monte Carlo tool. In: 2003 IEEE Nucl Sci Symp Conf Rec (IEEE Cat 03CH37515). 4:2549?53. https://doi.org/10.1109/nssmic.2003.1352
127. Ahmed AM, Chacon A, Rutherford H, Akamatsu G, Mohammadi A, Nishikido F, et al. A validated Geant4 model of a whole-body PET scanner with four-layer DOI detectors. Phys Med Biol. 2020;65:235051. https://doi.org/10.1088/1361-6560/abaa24.
128. Meo SL, Bennati P, Cinti MN, Lanconelli N, Navarria FL, Pani R, et al. A Geant4 simulation code for simulating optical photons in SPECT scintillation detectors. J Instrum. 2009;4:P07002?P07002. https://doi.org/10.1088/1748-0221/4/07/p07002.
129. Alfuraih A, Kadri O, Alzimami K. Investigation of SPECT/CT cardiac imaging using Geant4. Nucl Sci Tech. 2018;29:105. https://doi.org/10.1007/s41365-018-0435-8.
130. Wro?ska A, Kasper J, Ahmed AA, Andres A, Bednarczyk P, Gazdowicz G, et al. Prompt-gamma emission in GEANT4 revisited and confronted with experiment. Phys Med. 2021;88:250?61. https://doi.org/10.1016/j.ejmp.2021.07.018.
131. Pinto M, Dauvergne D, Freud N, Krimmer J, Létang JM, Testa E. Assessment of Geant4 prompt-gamma emission yields in the context of proton therapy monitoring. Front Oncol. 2016;6:10. https://doi.org/10.3389/fonc.2016.00010.
132. Silva RCL, Denyak V, Hoff G, Paschuk SA, Schelin HR, Setti JAP. GEANT4 simulation in proton medical imaging: a transport models comparison. Radiat Phys Chem. 2020;172:108814. https://doi.org/10.1016/j.radphyschem.2020.108814.
133. Silva RCL, Denyak V, Schelin HR, Hoff G, Paschuk SA, Setti JAP. GEANT4 simulation of exit energy in proton medical imaging. Radiat Phys Chem. 2020;167:108338. https://doi.org/10.1016/j.radphyschem.2019.05.028.
134. Vidal FP, Gabriela H. Geant4 validation on mammography applications. IEEE Nucl Sci Symp Conf Rec. 2008;2008:3497?8. https://doi.org/10.1109/nssmic.2008.4775089.
135. Jan S, Santin G, Strul D, Staelens S, Assié K, Autret D, et al. GATE: a simulation toolkit for PET and SPECT. Phys Med Biol. 2004;49:4543?61. https://doi.org/10.1088/0031-9155/49/19/007.
136. Sarrut D, Arbor N, Baudier T, Borys D, Etxebeste A, Fuchs H, et al. The OpenGATE ecosystem for Monte Carlo simulation in medical physics. Phys Med Biol. 2022;67:184001. https://doi.org/10.1088/1361-6560/ac8c83.
137. Wang H, Li X, Xu L, Kuang Y. PET/SPECT/spectral-CT/CBCT imaging in a small-animal radiation therapy platform: a Monte Carlo study?Part I: quad-modal imaging. Med Phys. 2024;51:2941?54. https://doi.org/10.1002/mp.17007.
138. Son K, Kim JS, Lee H, Cho S. IMAGING DOSE OF HUMAN ORGANS FROM kV-CBCT IN IMAGE-GUIDED RADIATION THERAPY. Radiat Prot Dosim. 2016. https://doi.org/10.1093/rpd/ncw285.
139. Liu Y, Li L, Huang G, Qiu W, Yang Y, Guo Y, et al. A preliminary study of dynamic interactive simulation and computational CT scan of the ideal alveolus model. Med Phys. 2024;51:601?11. https://doi.org/10.1002/mp.16773.
140. Shi M, Myronakis M, Hu Y-H, Morf D, Rottmann J, Berbeco R. A Monte Carlo study of the impact of phosphor optical properties on EPID imaging performance. Phys Medicine Biology. 2018;63:165013. https://doi.org/10.1088/1361-6560/aad647.
141. Shi M, Myronakis M, Jacobson M, Lehmann M, Ferguson D, Baturin P, et al. A rapid, accurate image simulation strategy for mega-voltage cone-beam computed tomography. Phys Medicine Biology. 2020;65:135004. https://doi.org/10.1088/1361-6560/ab868a.
142. Benhalouche S, Bert J, Autret A, Visvikis D, Pradier O, Boussion N. (2013) Imaging and Radiation Therapy: GATE Monte Carlo Simulation of a Megavolt Cone Beam CT. In: 2013 IEEE Nucl Sci Symp Med Imaging Conf (2013 NSSMIC). https://doi.org/10.1109/nssmic.2013.6829050.
143. Lee S, Gregor J, Osborne D. Development and validation of a complete GATE model of the siemens inveon trimodal imaging platform. Mol Imaging. 2013. https://doi.org/10.2310/7290.2013.00058.
144. Sarrut D, Ba?a M, Bardiès M, Bert J, Chauvin M, Chatzipapas K, et al. Advanced Monte Carlo simulations of emission tomography imaging systems with GATE. Phys Med Biol. 2021. https://doi.org/10.1088/1361-6560/abf276.
145. Razdev?ek G, Pestotnik R, Kri?an P, Korpar S, Consuegra D, Seljak A, et al. Exploring the potential of a cherenkov TOF PET scanner: a simulation study. IEEE Trans Radiat Plasma Med Sci. 2023;7:52?61. https://doi.org/10.1109/trpms.2022.3202138.
146. Saaidi R, Zeghari A, Moursli RCE. Monte Carlo simulation of two siemens biograph PET/CT system using GATE: Image quality performance. Radiat Phys Chem. 2024;218:111653. https://doi.org/10.1016/j.radphyschem.2024.111653.
147. Assié K, Breton V, Buvat I, Comtat C, Jan S, Krieguer M, et al. Monte Carlo simulation in PET and SPECT instrumentation using GATE. Nucl Instruments Methods Phys Res Sect Accel Spectrometers Detect Assoc Equip. 2004;527:180?9. https://doi.org/10.1016/j.nima.2004.03.117.
148. Kim M, Hong BH, Cho I, Park C, Min S-H, Hwang WT, et al. Design of a scintillator-based prompt gamma camera for boron-neutron capture therapy: comparison of SrI2 and GAGG using monte-carlo simulation. Nucl Eng Technol. 2021;53:626?36. https://doi.org/10.1016/j.net.2020.07.010.
149. Steinschaden D, Brunner SE, Dichtl H, Fuchs H, Georg D, Hirtl A, et al. Investigation of prompt ? ray emission for online monitoring in ion therapy. J Phys: Conf Ser. 2015;599:012042. https://doi.org/10.1088/1742-6596/599/1/012042.
150. Duarte IC, Caldeira L, Soares F, Silva JS, Janela F. GATE mammogram simulation of NCAT breast phantom. Berlin Heidelberg: Springer; 2010. p. 1482?5.
151. O?Connell J, Bazalova-Carter M. fastCAT: fast cone beam CT (CBCT) simulation. Med Phys. 2021;48:4448?58. https://doi.org/10.1002/mp.15007.
152. Scheins JJ, Lenz M, Pietrzyk U, Shah NJ, Lerche C. High-throughput, accurate Monte Carlo simulation on CPU hardware for PET applications. Phys Med Biol. 2021;66:185001. https://doi.org/10.1088/1361-6560/ac1ca0.
153. Torres-Tramon P, Vega-Acevedo N, Rannou FR. Multithreading GATE. IEEE Nucl Sci Symp Med Imaging Conf. 2010;1:3015?7. https://doi.org/10.1109/nssmic.2010.5874351.
154. Paredes-Pacheco J, López-González FJ, Silva-Rodríguez J, Efthimiou N, Niñerola-Baizán A, Ruibal Á, et al. SimPET?an open online platform for the Monte Carlo simulation of

realistic brain PET data. validation for 18F-FDG scans. Med Phys. 2021;48:2482?93. https://doi.org/10.1002/mp.14838.
155. Rannou FR, Vega-Acevedo N, Bitar ZE. A parallel computational model for GATE simulations. Comput Methods Programs Biomed. 2013;112:673?83. https://doi.org/10.1016/j.cmpb.2013.07.030.
156. Bert J, Perez-Ponce H, Bitar ZE, Jan S, Boursier Y, Vintache D, et al. Geant4-based Monte Carlo simulations on GPU for medical applications. Phys Med Biol. 2013;58:5593?611. https://doi.org/10.1088/0031-9155/58/16/5593.
157. Badal A, Badano A. Accelerating Monte Carlo simulations of photon transport in a voxelized geometry using a massively parallel graphics processing unit. Med Phys. 2009;36:4878?80. https://doi.org/10.1118/1.3231824.
158. Badal A, Badano A. Monte Carlo simulation of X-ray imaging using a graphics processing unit. Ieee Nucl Sci Symposium Conf Rec Nss Mic. 2009;2009:4081?4. https://doi.org/10.1109/nssmic.2009.5402382.
159. Herraiz JL, Lopez-Montes A, Badal A. MCGPU-PET: an open-source real-time Monte Carlo PET simulator. Comput Phys Commun. 2024;296:109008. https://doi.org/10.1016/j.cpc.2023.109008.
160. van der Heyden B, Uray M, Fonseca GP, Huber P, Us D, Messner I, et al. A Monte Carlo based scatter removal method for non-isocentric cone-beam CT acquisitions using a deep convolutional autoencoder. Phys Med Biol. 2020;65:145002. https://doi.org/10.1088/1361-6560/ab8954.
161. España S, Herraiz JL, Vicente E, Vaquero JJ, Desco M, Udias JM. PeneloPET, a Monte Carlo PET simulation tool based on PENELOPE: features and validation. Phys Med Biol. 2009;54:1723?42. https://doi.org/10.1088/0031-9155/54/6/021.
162. Salvat F, Fernández-Varea JM, Sempau J. PENELOPE-2006: A code system for Monte Carlo simulation of electron and photon transport. Citeseer; 2006. p. 7.
163. Voximetry. Torch. Available from: https://voximetry.com/our-software/
164. Solutions HM. Voxel dosimetry™. [cited 2024 Jul 15]. Available from: https://www.hermesmedical.com/our-software/dosimetry/voxel-dosimetry/
165. Capala J, Graves SA, Scott A, Sgouros G, James SS, Zanzonico P, et al. Dosimetry for radiopharmaceutical therapy: current practices and commercial resources. J Nucl Med. 2021;62:3S-11S. https://doi.org/10.2967/jnumed.121.262749.
166. Hippeläinen E, Tenhunen M, Sohlberg A. Fast voxel-level dosimetry for 177Lu labelled peptide treatments. Phys Med Biol. 2015;60:6685?700. https://doi.org/10.1088/0031-9155/60/17/6685.
167. Segars WP, Tsui BMW, Cai J, Yin F-F, Fung GSK, Samei E. Application of the 4-D XCAT phantoms in biomedical imaging and beyond. IEEE Trans Med Imaging. 2018;37:680?92. https://doi.org/10.1109/tmi.2017.2738448.
168. Lee C, Lodwick D, Hurtado J, Pafundi D, Williams JL, Bolch WE. The UF family of reference hybrid phantoms for computational radiation dosimetry. Phys Med Biol. 2010;55:339?63. https://doi.org/10.1088/0031-9155/55/2/002.
169. Geyer AM, O?Reilly S, Lee C, Long DJ, Bolch WE. The UF/NCI family of hybrid computational phantoms representing the current US population of male and female children, adolescents, and adults?application to CT dosimetry. Phys Med Biol. 2014;59:5225?42. https://doi.org/10.1088/0031-9155/59/18/5225.
170. Graff CG. A new open-source multi-modality digital breast phantom. Proc Spie. 2016. https://doi.org/10.1117/122216312.
171. de Sisternes L, Brankov JG, Zysk AM, Schmidt RA, Nishikawa RM, Wernick MN. A computational model to generate simulated three-dimensional breast masses. Med Phys. 2015;42:1098?118. https://doi.org/10.1118/1.4905232.
172. Sechopoulos I, Ali ESM, Badal A, Badano A, Boone JM, Kyprianou IS, et al. Monte Carlo reference data sets for imaging research: executive summary of the report of AAPM research committee task group 195. Med Phys. 2015;42:5679?91. https://doi.org/10.1118/1.4928676.
173. Rogers DWO, Mohan R. (2000) The Use of Computers in Radiation Therapy, XIIIth International Conference Heidelberg, Germany https://doi.org/10.1007/978-3-642-59758-9_44.
174. Gifford KA, Horton JL, Wareing TA, Failla G, Mourtada F. Comparison of a finite-element multigroup discrete-ordinates code with Monte Carlo for radiotherapy calculations. Phys Med Biol. 2006;51:2253?65. https://doi.org/10.1088/0031-9155/51/9/010.
175. Niu T, Xu L, Ren Q, Gao Y, Luo C, Teng Z, et al. UBES: unified scatter correction using ultrafast boltzmann equation solver for conebeam CT. Comput Biol Med. 2024;170:108045. https://doi.org/10.1016/j.compbiomed.2024.108045.
176. Maslowski A, Wang A, Sun M, Wareing T, Davis I, Star-Lack J. Acuros CTS: a fast, linear boltzmann transport equation solver for computed tomography scatter?Part I: core algorithms and validation. Med Phys. 2018;45:1899?913. https://doi.org/10.1002/mp.12850.
177. Wang A, Maslowski A, Messmer P, Lehmann M, Strzelecki A, Yu E, et al. Acuros CTS: a fast, linear boltzmann transport equation solver for computed tomography scatter?part II: system modeling, scatter correction, and optimization. Med Phys. 2018;45:1914?25. https://doi.org/10.1002/mp.12849.
178. Principi S, Lu Y, Liu Y, Wang A, Maslowski A, Wareing T, et al. Validation of a deterministic linear boltzmann transport equation solver for rapid CT dose computation using physical dose measurements in pediatric phantoms. Med Phys. 2021;48:8075?88. https://doi.org/10.1002/mp.15301.
179. Principi S, Wang A, Maslowski A, Wareing T, Jordan P, Schmidt TG. Deterministic linear boltzmann transport equation solver for patient-specific CT dose estimation: comparison against a Monte Carlo benchmark for realistic scanner configurations and patient models. Med Phys. 2020;47:6470?83. https://doi.org/10.1002/mp.14494.
180. Wang A, Maslowski A, Wareing T, Star-Lack J, Schmidt TG. A fast, linear boltzmann transport equation solver for computed tomography dose calculation (Acuros CTD). Med Phys. 2019;46:925?33. https://doi.org/10.1002/mp.13305.